β-Carboline Derivative-based Nickel (II) Complex as a Potential Antitumor Agent: Synthesis, Characterization, and Cytotoxicity †‡

Jing-Mei Yang[§a], Yan-Hong Zhu[§a], Sheng Chen[a], Xing Lu[a], Yi-Ming Wu[a], Feng-E Ma[a], Liang-Ping Li[a], Yang Yang[a], Zhen-Hao Shi[a], Kun-Yuan Huang[a], Xue Hong[a], Ping Jiang*[b], and Yan Peng*[a]

1 Materials and methods

1.1 Materials and methods

Primary antibodies against p-AKT, cyclin E, cyclin A and CDK2 were bought from AbcamInc (Cambridge, MA, USA). Primary antibodies cytochrome c, apaf-1, caspase-3, caspase-9 were purchased from Cell Signaling Technology (USA). MGC-803, Hep G2, T24, OS-RC-2, NCI-H460, SK-OV-3, and human normal liver cell lines HL-7702 were obtained from the American ATCC cell bank and the Shanghai Institute for Biological Science (China).. RNAse A, propidium iodide (PI) were purchased from Shanghai Sangon Biological Engineering Technology & Services (Shanghai, China). The CasPGLOW^{TM} Fluorescein Activite Caspase-3 Staining kit was purchased from BioVision. All chemical reagents were commercially available and received without further purification, unless noted specifically All the reagents were of analytical or HPLC grade where appropriate. Ultra-pure water was acquired from a Mill Q-plus system (Billerica, MA).Flow Cytometry (FCM) was recorded on FACS Aria Ⅱ Flow Cytometer (BD Biocsiences, San Jose, USA). Elemental analyses (C, H, N) were carried out on a Perkin Elmer Series II CHNS/O 2400 elemental analyser. UV-visible (UV-Vis) absorption spectra were obtained on a Perkin-Elmer Lambda45 UV-Visible spectrophotometer. Electrospray ionization mass spectrum

(ESI-MS) was recorded on a Bruker HCT Electrospray Ionization Mass Spectrometer.

The Stock solutions of the **4a** (2.0 mM) were made in DMSO. Further dilutions to working concentrations were made with corresponding buffer. All the spectroscopic experiments were performed at room temperature.

1.2 Synthesis and characterized

1.2.1 Synthesis

The synthetic route for the novel nickel (II) complex (**4a**) was outlined in Scheme 1. 5-methoxytryptamine (50 mmol) was dissolved in tetrahydrofuran (20 mL) and pyridine-2-carbaldehyde (0.63 mmol), and them the intermediate (**3**) was obtained. the intermediate (**3**) was dissolved in xylene (50 mL) and Catalyted by Pd / C (100 mg). Then 6-methoxy-1-pyridine-β-carboline (4) was obtained.

$Ni(NO_3)_2 \cdot 6H_2O$ (0.15mmol) and ligand of 1–pyridine -6-methoxy-β-carboline(0.1mmol) was added to a mixture of methanol(0.12 mL) and dimethylsulfoxide (0.01 mL) in a tube. The mixture was frozen by liquid N_2 and then the tube was sealed under a vacuum. The tube was allowed to heated to 80℃ for 72 hours, in an oven. The oven was slowly cooled to room temperature. Light yellow rod-like crystal of **4a** harvested. The product was filtered and washed successively with a small amount of water, methanol and dried to give the final product (Yield: 61%). The crystals with the regular shape and size were selected and analyzed by X-ray single crystal diffraction to determine this structure.

1.2.1 Characterization

Elemental analysis

Data for **4a**: $C_{35}H_{30}N_7O_6Ni$. Elemental analysis: Anal. Calc. (%): C, 59.77; H, 4.30; N, 13.94; O, 13.65. Found (%): C, 60.01; H, 4.28; N, 14.00; O, 13.64.

ESI-MS

Data for 4: ESI-MS (DMSO)：calcd for H($C_{17}H_{13}N_4O$) m/z 276.11. Found 276.11.

Data for **4a:** ESI-MS (DMSO): calcd for $C_{17}H_{13}N_4O_4Ni^+$ *m/z* 395.13. Found 395.13；calcd for $C_{34}H_{26}N_4O_5Ni^+$ *m/z* 670.13. Found 670.13；calcd for $C_{34}H_{25}N_6O_2Ni^+$ *m/z* 607.14. Found 607.14.

X-ray crystallography

The single crystals were mounted on glassfibres, and crystal data were collected on a Agilent SuperNova CCD diffractometer equipped with graphite monochromated Mo Kα radiation (λ=0.71073 Å) at room temperature. Absorption correction was applied by using the multiscan program SADABS.[1] The structures were solved with direct methods and refined using SHELX-97 programs.[2] The nonhydrogen atoms were located in successive difference Fourier synthesis. The final refinement was performed by full-matrix least squares methods with anisotropic thermal parameters for nonhydrogen atoms on F^2. The hydrogen atoms were added theoretically and riding on the concerned atoms. The crystallographic data and refinement details of the structures are summarized Table S1-S2.

1.3 Cell culture and treatment

Cell lines MGC-803, Hep G2, T24, OS-RC-2, NCI-H460, SK-OV-3, HL-7702 were obtained from American ATCC cell bank and the Institute of Biochemistry and

Cell Biology, Chinese Academy of Sciences (Shanghai, China). The cells were maintained in DMEM or RPMI1640 medium supplemented with 10% fetal calf serum, 100 units/mL ampicillin and 100 mg/mL streptomycin sulfate at 37 ℃ in a humidified atmosphere under 5% CO_2. **4a** were dissolved in DMSO at a concentration of 2.5 mM as a stock solution.

1.4 MTT assay

MGC-803, Hep G2, T24, OS-RC-2, NCI-H460, SK-OV-3, and human normal liver cell lines HL-7702 were seeded in 96-well plates (1.0×10^5/well) each with 90 μL. Cells were grown for 12.0 h before treatment to get 70% confluency and 10.0 μL of tested various concentrations of **4a** were added to each well. The final concentration of the tested **4**, **4a**, kept to 1.25, 2.5, 5, 10, 20 μM, respectively. The final content of DMSO was below 0.1%. After 48 h of incubation at 37 ℃ in a humidified atmosphere of 5% CO_2. Then 10 μL of a 5 mg/mL solution of MTT reagent was added to 100 μL of medium present in each well and cells were further incubated for 3h. The old medium was removed and 100 μL DMSO was added to each well. Formazan crystals were dissolved with 5 min of shaking, and absorption values were determined by microplate reader with 490/630 nm double wavelength measurement, blank group was regulated to zero baselines. **4** and **4a** doses were tested in parallel in quintuplicate. If the inhibition ratio exceeded 50% and the observed results were consistent with the natural biomorphic transformation of cells (such as shrinkage, floatage, and cytolysis), the initial antitumor efficacy was confirmed.

1.5 Cell cycle analysis by flow cytometry

The distribution of cell cycle phases was analyzed by flow cytometry. In the cell cycle assays, the MGC-803 cell line treated with 0.0 μM, 2.0 μM, 4.0 μM, 6.0 μM **4a** were harvested by trypsinization(EDTA) and rinsed with PBS. After centrifugation (800g, 5min), the pellet ($4x10^5$ cells) was suspended in 2.5 mL PBS. The cell suspension was then fixed by dropwise addition of 7.5 mL of precooled (4 ℃) 75% ethanol under violent shaking. Fixed samples were kept one day at -20 ℃ before use. For staining, cells were centrifuged (800g, 10min), resuspended in PBS (2.5 mL), digested with 500 μL RNAse A (250 μg/mL), then were incubated for 25 min at 37 ℃, and treated with 8 μL propidium iodide (PI) (100 μg/mL) for use. PI-positive cells were counted with a FACS Aria Ⅱ Flow Cytometer can fluorescence-activated cell sorter.

1.6 Apoptosis Analysis

Apoptosis was detected by flow cytometric analysis of annexin V staining. Annexin V-PE vs 7-AAD assay was performed as previously described. Briefly, adherent MGC-803 cells were harvested and suspended in the annexin-binding buffer (1×10^5 cells/mL). Then, cells were incubated with annexin V-PE and 7-AAD for 0.5 h at room temperature in the dark and immediately analyzed by flow cytometry. The data are presented as biparametric dot plots showing 7-AAD red fluorescence vs annexin V-PE orange red fluorescence.

1.7 Determination of caspase-3 activity by flow cytometric analysis

The measurement of caspase-3 activity was performed by CaspGLOW™ Fluorescein Active Caspase-3 Staining Kit. After a treatment with 2.0μM, 4.0μM,

6.0μM **4a** for 48 h, the inhibitor-treated cells and control cells were harvested at a density of 4 ×10^5 cells/mL in DMEM medium supplemented with 10% FBS. 300 μL each of the induced and control cultures were incubated with 1μL of FITC-DEVD-FMK (for caspase-3) for 30 min in a 37°C incubator with 5% CO_2. Flow cytometric analysis was performed using a FACSAriaⅡ flow cytometer (Becton Dickinson, San Jose, CA) equipped with a 488 nm argon laser. Results are represented as the percent change of the activity compared to the untreated control.

1.8 Measurement of reactive oxygen species (ROS) production

The level of ROS production was measured using the stain of DCFH-DA by flow cytometry.MGC-803 cells were incubated in 12-well culture plates at a cell density of 2 × 10^4 cells/well and exposed to 0.0 μM, 2 μM, 4μM, 6μM of **4a** for 48 h at 37 ºC. The cells were then loaded with 10 μM DCFH-DA and incubated at 37 ºC for 0.5 h the dark. After that, the cells were washed twice with serum-free cell culture medium, maintained in 300μL serum-free culture medium. The ROS generation was measured immediately by flow cytometry.

1.9 Measurement of intracellular calcium concentration ($[Ca^{2+}]_c$)

Intracellular Ca^{2+} concentration was analyzed by flow cytometry using Fluo-3 acetoxymethyl ester (Fluo-3 AM) staining. Briefly, MGC-803 cells were exposed to 0.0 μM, 2 μM, 4μM, 6μM of **4a**, stained with 5 μM Fluo-3 AM in dark for 30 min at 37 ºC, washed with PBS and measured immediately by flow cytometry

2 References

1 G.M. Sheldrick, SADABS. Version 2.05, University of Göttingen, Göttingen, Germany, 2002.

2 G.M. Sheldrick, SHELXS-97, Program for Solution of Crystal Structures, University of Göttingen, Göttingen, Germany, 1997.

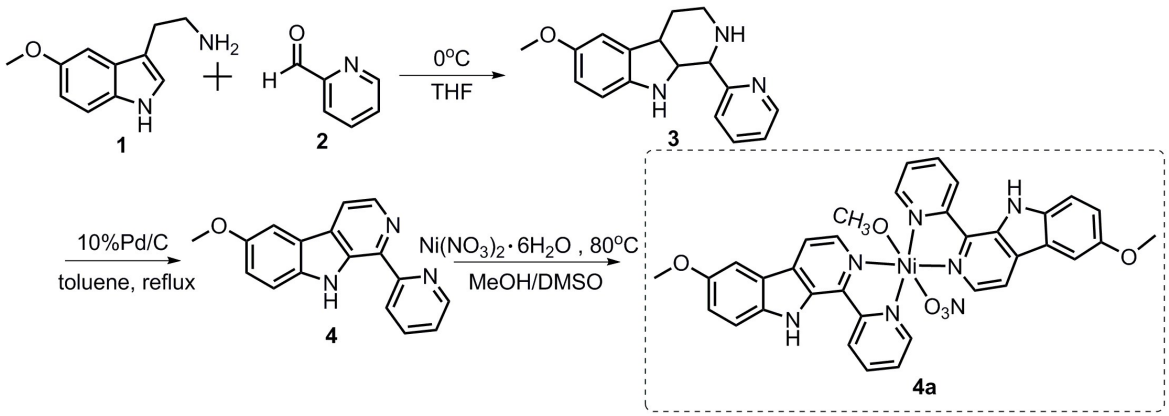

Scheme 1. Synthesis route of **4a**

Reagents and reaction conditions: (1) 0°C, THF; (2) 10% Pd/C, toluene. reflux; (3) $Ni(NO_3)_2$, MeOH/DMSO.

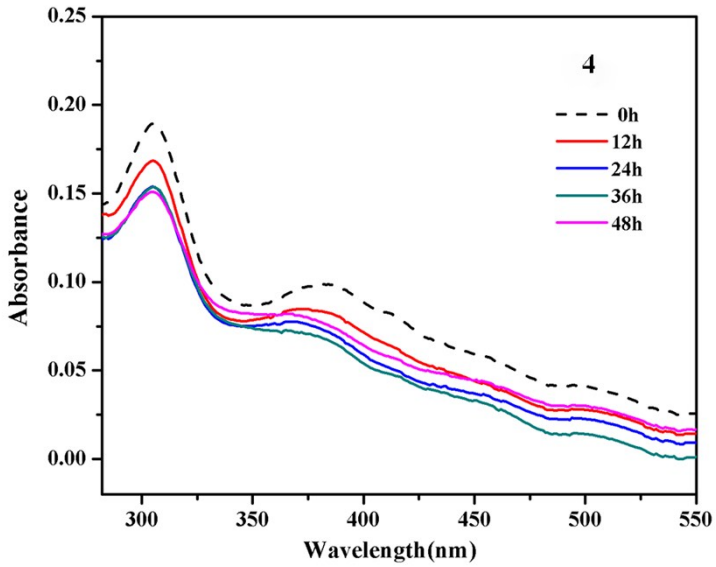

Fig. S1. UV-visible absorption spectra of **4**

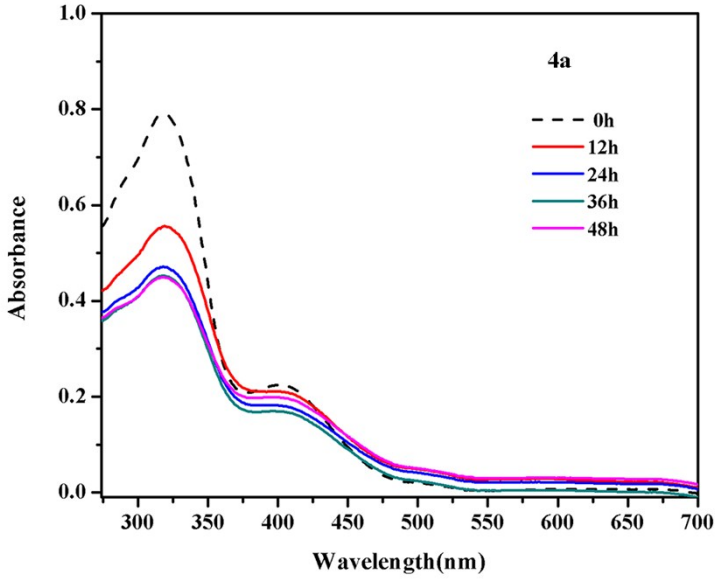

Fig. S2. UV-visible absorption spectra of **4a**

.

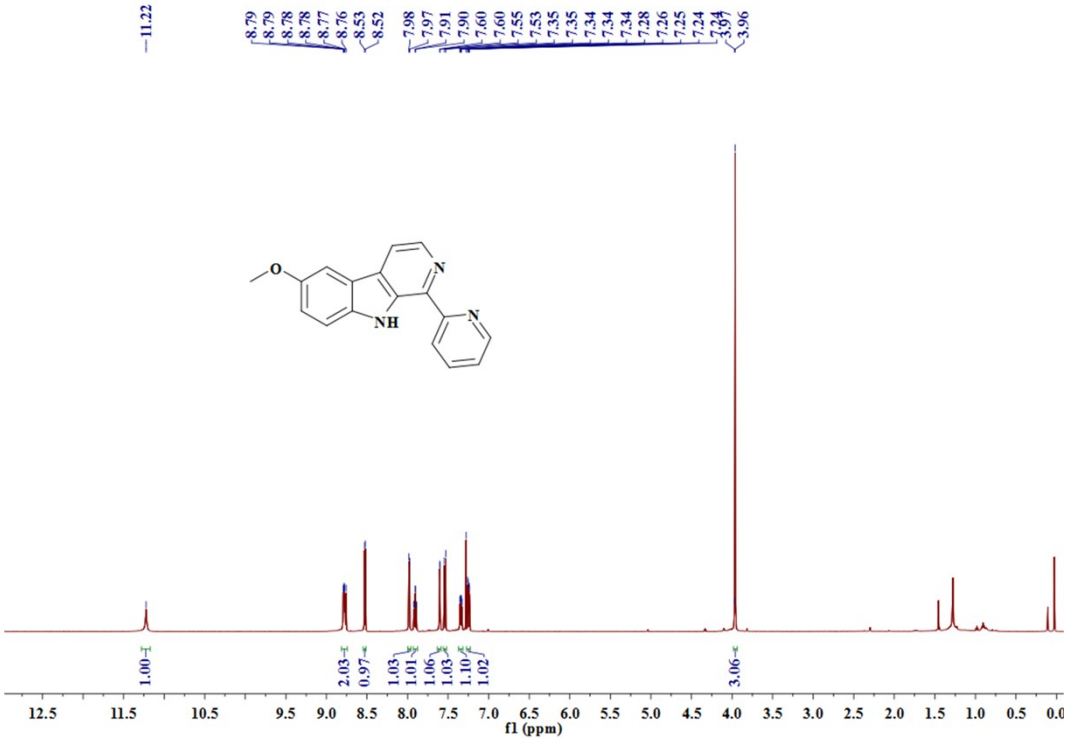

Fig. S3. ^{1}H NMR (500 MHz, DMSO-d_6) for **4**

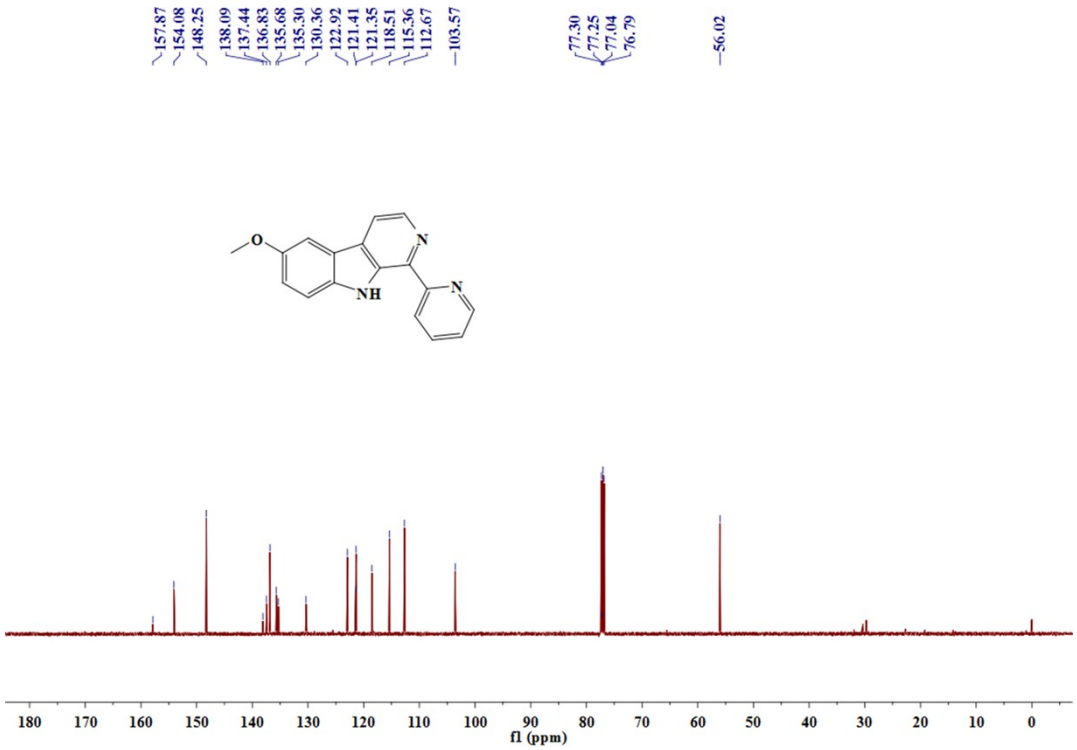

Fig. S4. ^{13}C NMR (500 MHz, DMSO-d_6) for **4**

Table S1. Selected bond lengths (Å) and bond angles (°) for **4**.

O1-C13	1.375(2)	N2-C6	1.338(2)
O1-C14	1.412(3)	N2-C7	1.353(2)
N1-C1	1.340(2)	N3-C10	1.371(2)
N1-C5	1.345(2)	N3-C17	1.386(2)
C13-O1-C14	118.06(16)	N2-C6-C10	120.05(15)
C1-N1-C5	117.17(17)	N2-C7-C8	124.71(16)
C6-N2-C7	119.03(16)	N3-C10-C6	130.99(15)
C10-N3-C17	108.92(14)	N3-C10-C9	108.75(14)
N1-C1-C2	124.3(2)	O1-C13-C12	124.33(17)
N1-C5-C4	122.13(16)	O1-C13-C15	114.64(16)
N1-C5-C6	116.77(15)	N3-C17-C11	109.23(14)
N2-C6-C5	117.23(15)	N3-C17-C16	129.83(16)

Table S2. Crystal Data and Structure Refinement Parameters for **4**.

	4
Empirical formula	$C_{17}H_{13}N_3O$
Formula weight	275.30
Temperature /K	296.15
Crystal system	Monoclinic
Space group	C2
Unit Cell Dimensions	a=17.435(2)Å α=90.00° b=19.1274(19)Å β=110.640°(13) c=22.985(3)Å γ=90.00°
Volume/Å^3	1378.4(7)
Z	4
ρ_{calc}/mg mm^{-3}	1.327
μ / mm^{-1}	0.086
F(000)	576
Crystal size / mm^3	0.30 × 0.15 × 0.08
θ range for data Collection (°)	3.54 to 52.74°
Index ranges	-22 ⩽ h ⩽ 22, -8 ⩽ k ⩽ 8, -16 ⩽ l ⩽ 16
Reflections collected	7860
Independent reflections	2793[R(int) = 0.0322]
Goodness-of-fit on F^2	1.059
Final R indexes [I>2σ(I)]	R1 = 0.0348 wR2 = 0.0882
Final R indexes [all data]	R1 = 0.0435 wR2 = 0.0945

[a] $R_1 = \Sigma\, ||F_o| - |F_c||/\Sigma|F_o|$; [b] $wR_2 = [\Sigma w(F_o^2 - F_c^2)^2/\Sigma w(F_o^2)^2]^{1/2}$.

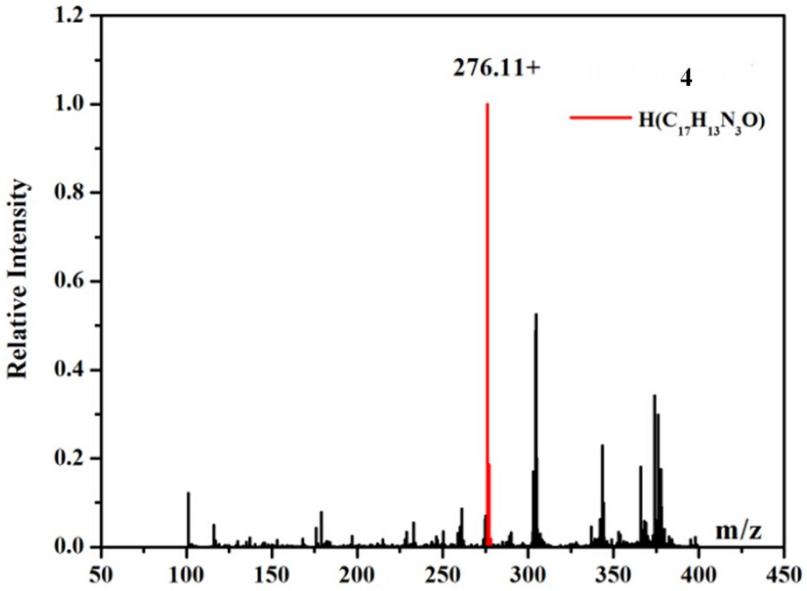

Fig. S5. MS-EI spectrum of **4**.

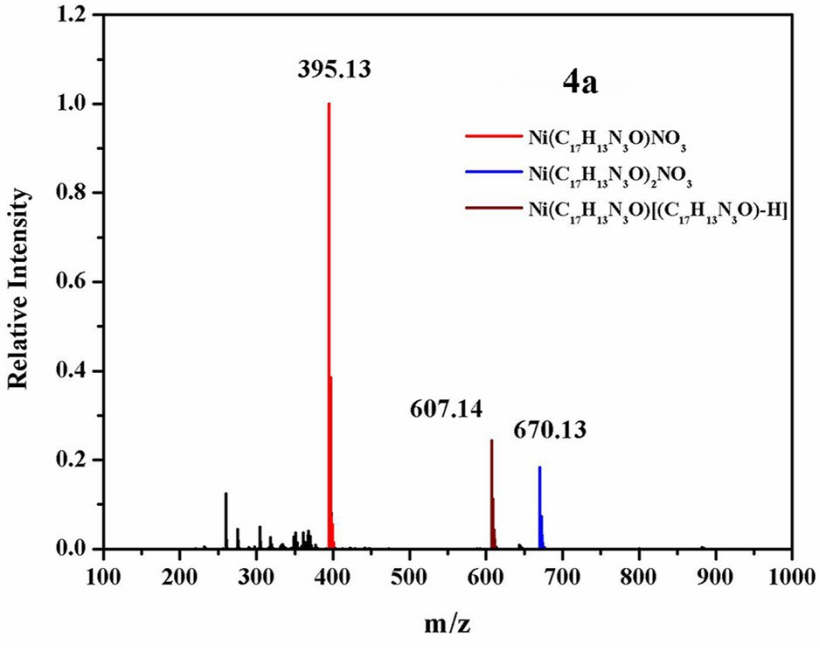

Fig. S6. MS-EI spectrum of **4a**.

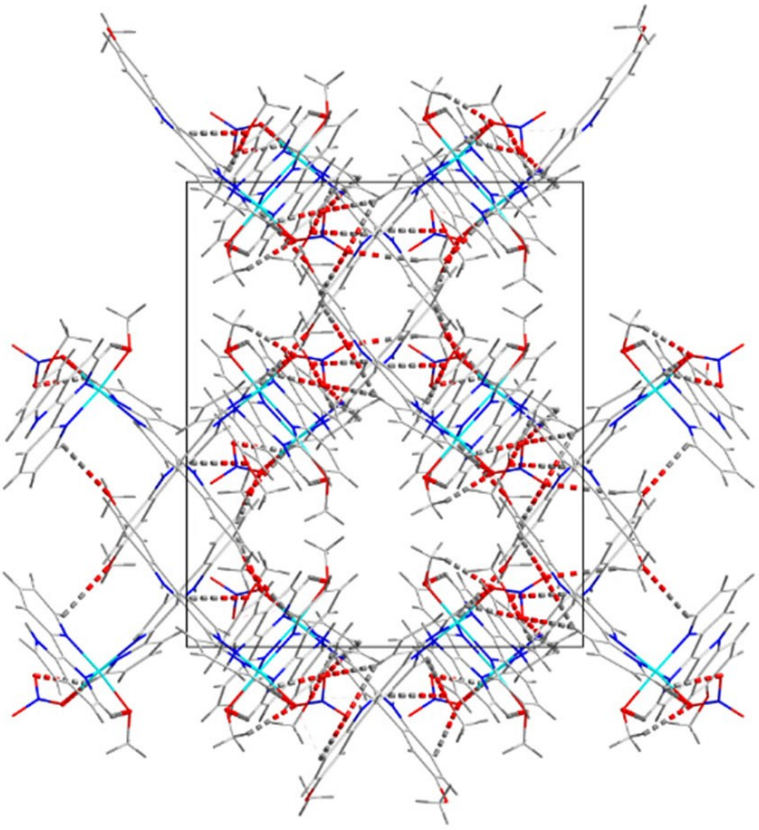

Fig. S7. Cell packing diagram of the complex **4a** along a axis.

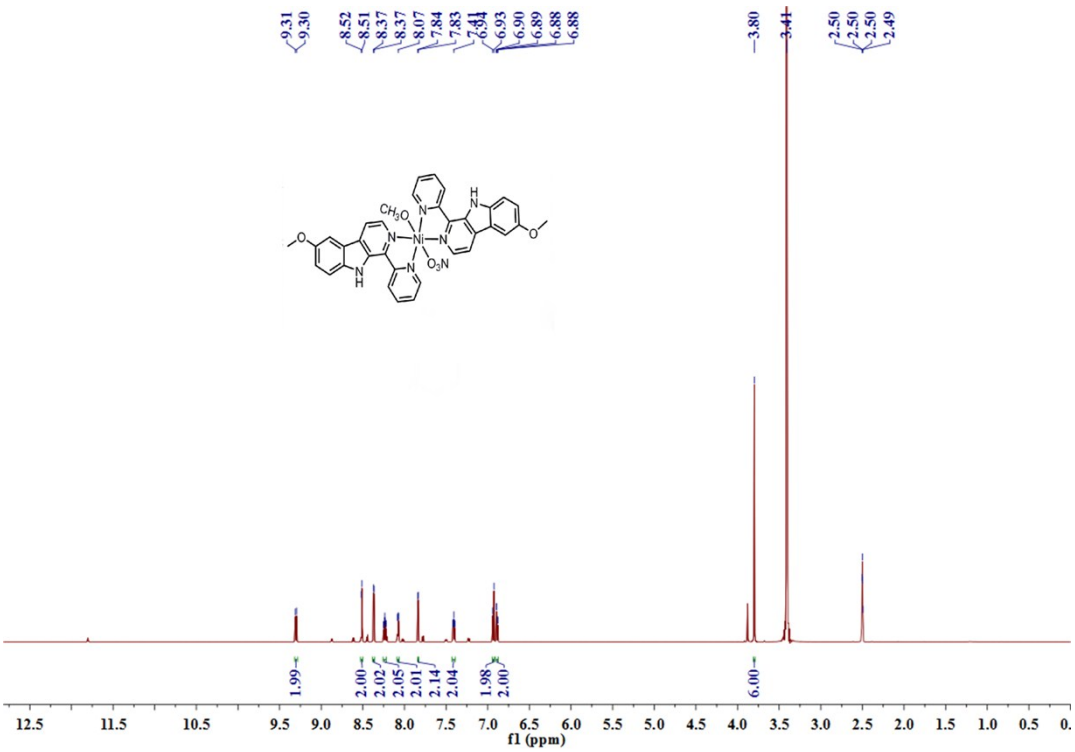

Fig. S8. ^{1}H NMR (500 MHz, DMSO-d_6) for **4a**

Table S3. Selected bond lengths (Å) and bond angles (°) for **4a**.

Ni(1)—N(11)	2.098 (14)	Ni(1)—N(8)	2.052 (16)
Ni(1)—N(7)	2.055 (16)	Ni(1)—O(12)	2.084 (13)
Ni(1)—N(10)	2.034 (16)	Ni(1)—O(9)	2.121 (13)
Ni(2)—N(5)	2.073 (15)	Ni(2)—N(2)	2.038 (15)
Ni(2)—N(4)	2.010 (14)	Ni(2)—O(8)	2.082 (16)
Ni(2)—N(1)	2.124 (15)	Ni(2)—O(5)	2.129 (13)
Ni(2)—H(2)	3.1 (12)	O(8)—Ni(2)—H(2)	22 (10)
O(5)—Ni(2)—H(2)	108 (10)	O(5)—Ni(2)—N(1)	96.6 (7)
N(1)—Ni(2)—H(2)	88 (10)	O(8)—Ni(2)—N(1)	88.5 (6)
O(8)—Ni(2)—O(5)	85.6 (6)	N(4)—Ni(2)—H(2)	158 (2)
N(4)—Ni(2)—O(5)	91.6 (6)	N(4)—Ni(2)—N(1)	101.0 (6)
N(4)—Ni(2)—O(8)	170.4 (5)	N(4)—Ni(2)—N(2)	91.6 (6)
N(4)—Ni(2)—N(5)	77.7 (6)	N(2)—Ni(2)—H(2)	70 (10)
N(2)—Ni(2)—O(5)	175.3 (6)	N(2)—Ni(2)—N(1)	79.4 (6)
N(2)—Ni(2)—O(8)	91.8 (6)	N(2)—Ni(2)—N(5)	93.4 (5)
N(5)—Ni(2)—H(2)	91 (10)	N(5)—Ni(2)—O(5)	90.6 (6)
N(5)—Ni(2)—N(1)	172.7 (6)	N(5)—Ni(2)—O(8)	93.1 (6)
N(10)—Ni(1)—O(9)	96.8 (6)	N(10)—Ni(1)—O(12)	83.6 (6)
N(10)—Ni(1)—N(7)	101.4 (7)	N(10)—Ni(1)—N(8)	174.9 (6)
N(10)—Ni(1)—N(11)	77.9 (6)	O(12)—Ni(1)—O(9)	85.9 (6)
O(12)—Ni(1)—N(11)	88.2 (5)	N(7)—Ni(1)—O(9)	93.8 (5)
N(7)—Ni(1)—O(12)	175.0 (6)	N(7)—Ni(1)—N(8)	80.5 (7)
N(7)—Ni(1)—N(11)	92.4 (5)	N(8)—Ni(1)—O(9)	87.8 (5)
N(8)—Ni(1)—O(12)	94.4 (6)	N(8)—Ni(1)—N(11)	97.3 (5)
N(11)—Ni(1)—O(9)	172.5 (5)		

Table S4. Crystal Data and Structure Refinement Parameters for **4a**.

	4a
Empirical formula	$C_{72}H_{65}N_{16}Ni_2O_{20}$
Formula weight	1591.82
Temperature /K	293(2)

Crystal system	Monoclinic
Space group	Ia
Unit Cell Dimensions	a=17.435(2)Å α=90.00° b=19.1274(19)Å β=110.640°(13) c=22.985(3)Å γ=90.00°
Volume/Å^3	7173.1(14)
Z	4
ρ_{calc}/mg mm^{-3}	1.474
μ / mm^{-1}	0.612
F(000)	3300
Crystal size / mm^3	0.30 × 0.15 × 0.08
θ range for data Collection (°)	6.64 to 52.74°
Index ranges	−18 ≤ h ≤18 −23 ≤ k ≤ 23 −27 ≤ l ≤ 28
Reflections collected	18952
Independent reflections	11081[$R_{(int)}$=0.0657]
Goodness-of-fit on F^2	0.985
Final R indexes [I>2σ(I)]	R_1=0.0733 ωR_2=0.1292
Final R indexes [all data]	R_1=0.1813 ωR_2=0.1877

[a] $R_1 = \Sigma\ ||F_o| - |F_c||/\Sigma|F_o|$; [b] $wR_2 = [\Sigma w(F_o^2 - F_c^2)^2/\Sigma w(F_o^2)^2]^{½}$.

Table S5. Inhibitory rates (%) and IC_{50} (μM) values of **4a, 4** and cisplatin towards seven selected cell lines for 48 h.

	T24 Inhibitory rates (%)	MGC-803 Inhibitory rates (%)	OS-RC-2 Inhibitory rates (%)	NCI-H-460 Inhibitory rates (%)	SK-OV-3 Inhibitory rates (%)	Hep G2 Inhibitory rates (%)	HL-7702 Inhibitory rates (%)
4a	82.48±0.02	92.39±0.00	82.48±0.01	81.81±0.00	72.80±0.02	91.10±0.00	68.99±0.22
4	41.90±0.03	53.49±0.11	56.49±0.11	32.42±0.02	24.79±0.01	57.94±0.14	72.59±0.32
cisplatin	74.61±0.33	52.77±0.21	49.15±0.01	46.58±0.04	52.13±0.02	55.64±0.01	25.04±0.14

	T24 $IC_{50}(\mu M)$	MGC-803 $IC_{50}(\mu M)$	OS-RC-2 $IC_{50}(\mu M)$	NCI-H-460 $IC_{50}(\mu M)$	SK-OV-3 $IC_{50}(\mu M)$	Hep G2 $IC_{50}(\mu M)$	HL-7702 $IC_{50}(\mu M)$
4a	9.51±2.76	3.77±0.26	11.35±0.45	15.10±0.71	15.03±0.23	4.43±1.00	14.56±0.13
4	＞20	18.13±0.41	17.66±1.17	＞20	＞20	14.33±0.47	10.8±0.51
cisplatin	11.00±0.20	17.57±0.23	＞20	＞20	17.64±0.31	17.73±0.42	＞20

Noted: Results represent as ‘mean ± SD’ of at least three independent experiments. SD represents the standard deviation. The inhibition rates of **4a, 4** were achieved at concentration of 20 μM